



The long noncoding RNA Blnc1 orchestrates homeostatic adipose tissue remodeling to preserve metabolic health

Xu-Yun Zhao¹, Siming Li¹, Jennifer L. DelProposto², Tongyu Liu¹, Lin Mi¹, Cara Porsche², Xiaoling Peng¹, Carey N. Lumeng², Jiandie D. Lin^{1,*}

ABSTRACT

Objective: Long noncoding RNAs (lncRNAs) are emerging as powerful regulators of adipocyte differentiation and gene expression. However, their significance in adipose tissue metabolism and physiology has not been demonstrated *in vivo*. We previously identified Blnc1 as a conserved lncRNA regulator of brown and beige adipocyte differentiation. In this study, we investigated the physiological role of Blnc1 in thermogenesis, adipose remodeling and systemic metabolism.

Methods: We generated fat-specific Blnc1 transgenic and conditional knockout mouse strains and investigated how adipocyte Blnc1 levels are causally linked to key aspects of metabolic health following diet-induced obesity. We performed studies using cultured adipocytes to establish cell-autonomous role of Blnc1 in regulating adipocyte gene programs.

Results: Blnc1 is highly induced in both brown and white fats from obese mice. Fat-specific inactivation of Blnc1 impairs cold-induced thermogenesis and browning and exacerbates obesity-associated brown fat whitening, adipose tissue inflammation and fibrosis, leading to more severe insulin resistance and hepatic steatosis. On the contrary, transgenic expression of Blnc1 in adipose tissue elicits the opposite and beneficial metabolic effects, supporting a critical role of Blnc1 in driving adipose adaptation and homeostatic remodeling during obesity. Mechanistically, Blnc1 cell-autonomously attenuates proinflammatory cytokine signaling and promotes fuel storage in adipocytes through its protein partner Zbtb7b.

Conclusions: This study illustrates a surprisingly pleiotropic and dominant role of lncRNA in driving adaptive adipose tissue remodeling and preserving metabolic health.

© 2018 Published by Elsevier GmbH. This is an open access article under the CC BY-NC-ND license (<http://creativecommons.org/licenses/by-nc-nd/4.0/>).

Keywords lncRNA; Adipose tissue remodeling; Brown fat; White fat; Whitening; Inflammation; Obesity

1. INTRODUCTION

Adipose tissue is a remarkably versatile organ central to metabolic homeostasis. White adipose tissue (WAT) stores lipids, secretes endocrine factors, and integrates immune and metabolic signals [1–6], whereas brown adipose tissue (BAT) oxidizes fuels to generate heat and is emerging as a source of important endocrine factors [7–11]. WAT exhibits enormous plasticity in its storage capacity. In response to chronic overnutrition, WAT undergoes dramatic expansion through adipocyte hypertrophy and recruitment of newly generated adipocytes [3,12–14]. However, this healthy fat expansion often transitions into a pathological state of adipose tissue remodeling that is associated with activation of a proinflammatory immunological milieu in rodent and human obesity. Persistent adipocyte stress and injury activate wound repair response in adipose tissue, leading to fibrosis in WAT. The mechanisms underlying the adaptive healthy fat expansion and its switch to adipose tissue dysfunction in obesity remain elusive.

Brown fat contains high mitochondrial content and generates heat through uncoupling protein 1 (UCP1)-dependent and independent mechanisms [15]. Brown fat thermogenesis is critical for defense against cold temperature and obesity in rodents. Genetic and pharmacological activation of brown fat thermogenesis increased energy expenditure, reduced adiposity, and improved glucose and lipid parameters [16–18]. Recent studies demonstrate that brown fat undergoes pronounced whitening in obesity, in which brown adipocytes acquire molecular and morphological features of white adipocytes [19–21]. This aberrant remodeling of brown fat may contribute to impaired thermogenesis and metabolic dysfunction. Beyond thermogenesis, brown fat influences metabolic physiology through its secretion of endocrine factors such as Neuregulin 4 (Nrg4), which attenuates hepatic lipogenesis and liver injury [22–24]. Several transcriptional regulators have been implicated in the control of brown and beige fat development and maintenance, including PR Domain Containing 16 (PRDM16) [8,25,26], Early B-cell Factor 2 (EBF2) [27],

¹Life Sciences Institute and Department of Cell & Developmental Biology, University of Michigan Medical Center, Ann Arbor, MI 48109, USA ²Department of Pediatrics and Communicable Diseases, University of Michigan Medical Center, Ann Arbor, MI 48109, USA

*Corresponding author. 5437 Life Sciences Institute, University of Michigan, 210 Washtenaw Avenue, Ann Arbor, MI 48109, USA. Fax: +734 615 0495. E-mail: jclin@umich.edu (J.D. Lin).

Received May 13, 2018 • Revision received June 1, 2018 • Accepted June 6, 2018 • Available online 8 June 2018

<https://doi.org/10.1016/j.molmet.2018.06.005>

Interferon Regulatory Factor-4 [28], Zinc-Finger Protein 516 [29], PPAR γ coactivator-1 α (PGC-1 α), Euchromatic Histone-lysine N-methyltransferase 1 (EHMT1) [26,30] and zinc finger and BTB domain containing 7b (Zbtb7b) [31].

Recent studies have implicated long noncoding RNAs (lncRNAs) as a new class of non-protein regulators of adipocyte biology [32]. A notable feature of lncRNA expression is that many exhibit restricted tissue distribution and are highly regulated by developmental and hormonal signals [33–36]. Global transcriptomic analyses have led to the identification of highly inducible lncRNAs during brown and white adipocyte differentiation [37–39]. Among these, brown fat lncRNA 1 (Blnc1) was identified as a conserved BAT-enriched lncRNA that promotes differentiation of cultured brown and beige adipocytes. Blnc1 forms ribonucleoprotein transcriptional complexes with the transcription factors EBF2 and Zbtb7b and heterogeneous nuclear ribonucleoprotein U (hnRNP) to stimulate thermogenic gene expression [31,39,40]. Despite this, the role of lncRNAs in adipose tissue remodeling and metabolic physiology has not been fully established. Here we show that fat-specific inactivation of Blnc1 accelerates brown fat whitening and impairs homeostatic fat expansion during high-fat diet (HFD) feeding, leading to adipose tissue inflammation, insulin resistance and hepatic steatosis. Adipocyte-specific transgenic expression of Blnc1 elicited the opposite and beneficial metabolic effects. Mechanistically, Blnc1 cell-autonomously attenuates proinflammatory cytokine signaling in adipocytes through its protein partner Zbtb7b. This study illustrates a surprisingly powerful role of lncRNA in orchestrating adipocyte adaptation to obesity and maintaining systemic metabolic health.

2. METHODS

2.1. Animal studies

All animal studies were performed according to procedures approved by the University Committee on Use and Care of Animals at the University of Michigan. Mice were maintained in 12/12 h light/dark cycles and fed regular rodent chow or high-fat diet (D12492, Research Diets). Wild type C57BL/6J mice (JAX stock #000664) and floxed STOP-Cas9 knockin mice (JAX stock #024857) was purchased from the Jackson Laboratory.

For the generation of Blnc1-single-guide RNA transgenic (sgRNA-TG) mice, we designed two sgRNAs flanking the Blnc1 gene, which contains a single exon using a CRISPR design web tool (<http://crispr.mit.edu/>) [43]. Each sgRNA targeting Blnc1 was cloned at downstream of U6 promoter and the tandem U6-sgRNA cassette with two sgRNAs was pronuclear microinjected into the fertilized egg. Then, we crossed floxed STOP-Cas9 knockin mice with Adiponectin-CRE transgenic mice and Blnc1-sgRNA TG mice to generate floxed STOP-Cas9, Adiponectin-CRE and Blnc1 sgRNA triple TG mice, which contain the Blnc1 deletion allele in adipose tissue. For Blnc1 adipose specific transgenic mice, full-length Blnc1 sequence was cloned downstream of a murine aP2 promoter [44]. Transgenic mice were generated by pronuclear microinjection. Seven independent founders were identified and crossed with C57BL/6 mice to generate stable transgenic lines.

For cold acclimation, mice were maintained in a temperature-controlled chamber. The temperature decreased 4 °C every day until reaching 10 °C for five more days before tissue harvest. For histology, tissues were dissected and fixed in 10% formalin overnight at 4 °C and subjected to paraffin embedding and H&E staining. Sirius Red staining was processed as previously described [45]. Hydroxyproline level in the eWAT was measured using a Hydroxyproline Colorimetric Assay Kit (BioVision).

2.2. Cell culture

C3H10T1/2 cells expressing vector/Blnc1/Zbtb7b or scramble/Blnc1 shRNA were maintained in DMEM supplemented with 10% fetal bovine serum (FBS). Confluent preadipocytes were subjected for differentiation by adding an induction medium containing 0.5 mM IBMX, 125 μ M indomethacin, 1 μ M dexamethasone, 20 nM insulin and 1 nM T3. Cells were switched to differentiation medium (DMEM, 10% FBS, 20 nM insulin and 1 nM T3) after two days. TNF α treatment was performed in the fully differentiated adipocytes. Protein level of IL-6 and CCL5 in the conditional medium was measured using ELISA kits (R&D system).

2.3. Metabolic analyses

For Glucose Tolerant Test (GTT), mice were fasted overnight (16 h) and injected intraperitoneally (IP) with a glucose solution at a dose of 1.0 g/kg body weight. For Insulin Tolerant Test (ITT), mice were pre-fasted for 4 h and IP injected with insulin at a dose of 1 U/kg body weight. Blood glucose concentrations were measured before and 20, 45, 90 and 120 min after glucose or insulin injection. Liver triglyceride was extracted and measured as previously described [46]. Plasma insulin was measured using an ELISA kit (CrystalChem).

2.4. Microarray analysis

Total RNA was isolated from white adipose tissues of WT and Blnc1 Tg mice after HFD feeding. Gene expression profiling was performed using Mouse Gene ST 2.1 plates. We used a cutoff of normalized array values (log₂-transformed values > 6.0) to enrich for transcripts present in white fat. We performed student's t-test to identify transcripts exhibiting significant differences of over 1.6-fold for Tg groups compared to WT. Gene Ontology analysis was performed using the Database for Annotation, Visualization and Integrated Discovery (DAVID, available at <http://david.abcc.ncifcrf.gov>).

2.5. Adipose tissue explant culture

Epididymal WAT (eWAT) from WT and Blnc1 Tg mice was dissected and transferred to a culture dish with 10 ml DMEM. Fat pad was cut into approximately 4 mm pieces and washed sequentially with 10 \times volume PBS and DMEM. Equal number of fat pieces were transferred into six-well plates with serum-free M199 media (1 nM insulin, 1 nM dexamethasone), and cultured for 24 h before TNF α treatment. Following treatments, fat tissues were collected and processed gene expression and immunoblotting analyses.

2.6. Gene expression analyses

Total RNA from differentiated adipocytes was extracted using TRIzol method following manufacturer instructions. Total tissue RNA was isolated using PureLink RNA isolation kit (ThermoFisher). For RT-qPCR, 2 μ g of RNA was reverse-transcribed using MMLV (Invitrogen) followed by qPCR using SYBR Green (Life Technologies). Relative mRNA expression was normalized to the expression of ribosomal protein 36B4.

2.7. Immunoblotting analysis

Total cell lysates were prepared in a lysis buffer containing 50 mM Tris-HCl (pH = 7.8), 137 mM NaCl, 10 mM NaF, 1 mM EDTA, 1% Triton X-100, 10% glycerol, and the protease inhibitor cocktail (Roche) after three freeze/thaw cycles. Tissue lysates were prepared by homogenizing in a buffer containing 50 mM Tris (pH = 7.6), 130 mM NaCl, 5 mM NaF, 25 mM β -glycerophosphate, 1 mM sodium orthovanadate, 10% glycerol, 1% Triton X-100, 1 mM DTT, 1 mM PMSF and the protease inhibitor cocktail. The antibodies used are: anti-UCP1 (UCP11-A) from Alpha Diagnostic; anti-Tubulin (T6199,

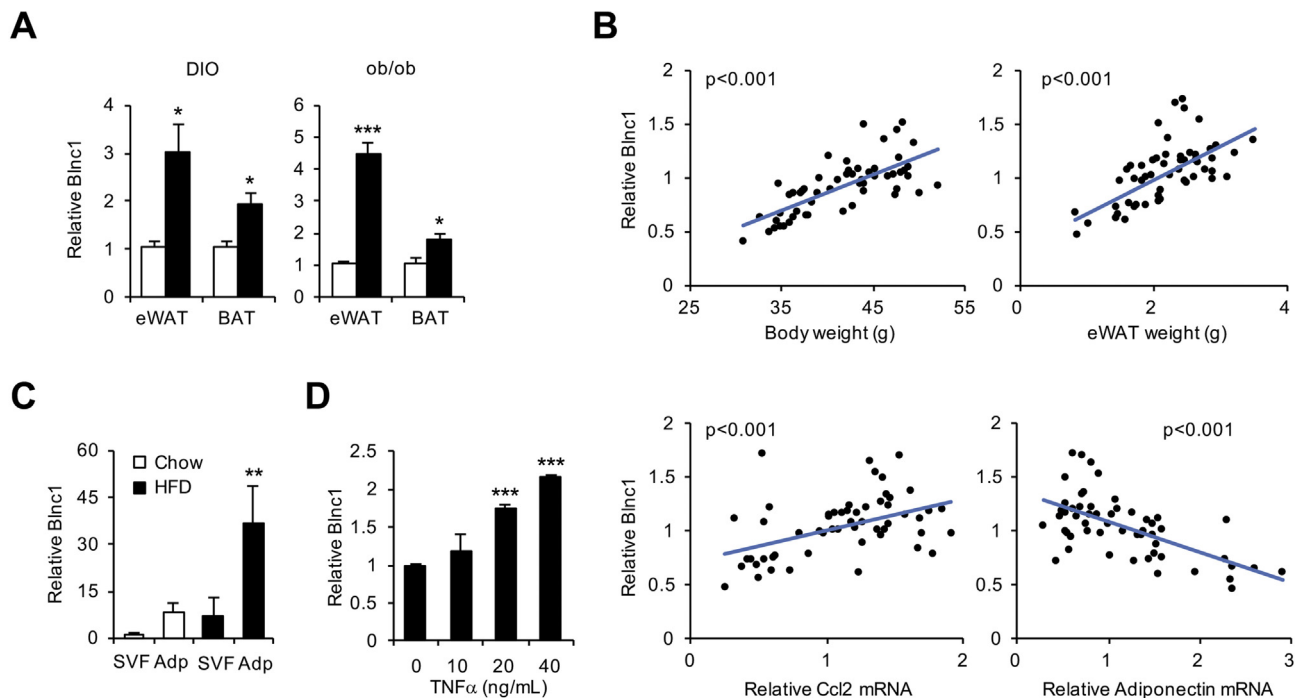


Figure 1: Blnc1 expression in adipocyte is linked to obesity and inflammatory cytokine. (A) qPCR analysis of Blnc1 expression in eWAT and BAT from lean (open, $n = 5$) and obese (filled, $n = 6$) mice. Data represent mean \pm SEM. * $p < 0.05$, *** $p < 0.001$ obese vs. lean, two-tailed unpaired Student's t -test. (B) Correlation between eWAT Blnc1 expression and body weight, eWAT weight, and Ccl2 or adiponectin mRNA levels in HFD-fed mice. (C) qPCR analysis of Blnc1 expression in stromal vascular fraction (SVF) and adipocyte fraction (Adp) isolated from eWAT from lean (open) or HFD-fed (filled) mice. Data represent mean \pm SD ($n = 4$). *** $p < 0.001$, SVF vs. Adp, two-way ANOVA. (D) qPCR analysis of Blnc1 expression in differentiated C3H10T1/2 cells treated with TNF α at indicated dose for 24 h. Data represent mean \pm SD ($n = 3$). *** $p < 0.001$, TNF α vs. veh, one-way ANOVA.

Sigma); anti-phospho-TBK1 (S172) (5483), anti-TBK1 (3013), anti-phospho-NF- κ B-p65 (S536) (3033), anti-NF- κ B-p65 (8242), anti-phospho-p38 MAPK (T180/Y182) (9215), anti-p38 MAPK (9212) and anti-IKKe (3416) are from Cell Signaling Technology.

2.8. Statistical analysis

Statistical analysis was performed using GraphPad Prism 7. Statistical differences were evaluated using two-tailed unpaired Student's t -test for comparisons between two groups, or analysis of variance (ANOVA) and appropriate *post hoc* analyses for comparisons of more than two groups. Two-way ANOVA with multiple comparisons was used for statistical analysis of Body weight, GTT, ITT studies. A p value of less than 0.05 (* $p < 0.05$, ** $p < 0.01$, and *** $p < 0.001$) was considered statistically significant. Statistical methods and corresponding p values for data shown in each panel were included in the figure legends.

2.9. Data and software availability

Microarray data files have been deposited at the Gene Expression Omnibus (www.ncbi.nlm.nih.gov/geo/) with accession number GSE111865.

3. RESULTS

3.1. Adipose Blnc1 expression is elevated in obesity

Several lncRNAs have emerged as potent regulators of adipocyte gene expression and differentiation [37–39]. However, the significance of these lncRNAs in adipose tissue metabolism and physiology has not been established. Our previous studies demonstrate that Blnc1 is a

conserved and inducible lncRNA that promotes thermogenic adipocyte differentiation [39,40]. To explore its role in adipose tissue biology, we first examined whether Blnc1 expression in brown and white adipose tissue is altered by obesity in mice. While BAT Blnc1 expression was moderately elevated in obesity, to our surprise, its expression in epididymal WAT (eWAT) was markedly induced in HFD-fed obese and leptin-deficient (ob/ob) mice (Figure 1A). In a cohort of HFD-fed C57BL6/J mice exhibiting varying degree of diet-induced obesity, eWAT Blnc1 expression was strongly associated with weight gain and eWAT mass (Figure 1B). In addition, Blnc1 expression was positively and inversely correlated with Chemokine (C–C motif) ligand 2 (Ccl2) and Adiponectin mRNA levels, respectively. This obesity-associated induction of Blnc1 is restricted to adipocytes, but not stromal vascular fraction (Figure 1C). Blnc1 expression was significantly induced in differentiated C3H10T1/2 adipocytes in response to tumor necrosis factor alpha (TNF α) treatments (Figure 1D). These observations raise the possibility that increased Blnc1 may contribute to adipose tissue dysfunction in obesity, or alternatively, Blnc1 may facilitate adipose adaptation to nutritional stress and preserve metabolic health.

3.2. Blnc1 is required for cold-induced thermogenesis and white fat browning

To critically assess the role of Blnc1 in the regulation of adipocyte biology, we developed a CRISPR/Cas9-based method to conditionally inactivate Blnc1 in adipose tissue. We first generated transgenic mouse strains expressing two single guide RNAs (sgRNAs) flanking Blnc1, a single-exon gene, under the control of U6 promoter (Supplementary Fig. 1A). We crossed the Blnc1 sgRNA transgenic mice

with a mouse strain expressing Cas9 specifically in adipose tissue (Adiponectin-CRE; floxed STOP-Cas9 knockin). As expected, the triple transgenic mice exhibited efficient Cas9-mediated deletion of the *Blnc1* gene in BAT, iWAT and eWAT. These adipocyte-specific *Blnc1* knockout (AKO) mice had markedly diminished *Blnc1* expression in adipose tissue compared to control (Supplementary Fig. 1B–C). In contrast, *Blnc1* levels in SVF remained similar between two groups. We previously demonstrated that iWAT *Blnc1* expression is induced by CL-316,243, a β -selective adrenergic agonist [39]. Consistently, iWAT and BAT expression of *Blnc1* was strongly stimulated in response to cold acclimation (Figure 2A). To determine whether *Blnc1* is required for white fat browning, we performed cold acclimation studies where we gradually decreased housing temperature from 23 °C to 10 °C over a period of five days. H&E staining indicated that BAT histology remained similar between two groups. In contrast, the appearance of beige adipocytes with multilocular lipid droplets in iWAT was greatly diminished by *Blnc1* inactivation (Figure 2B). UCP1 protein levels were

lower in both BAT and iWAT from AKO mice (Figure 2C). While mRNA levels of *Ppargc1a*, *Ebf2* and *Prdm16* remained largely unaffected by *Blnc1* inactivation, expression of thermogenic fat markers, such as *Ucp1*, *Cidea*, *Cox8b* and *Ppara α* , was significantly decreased (Figure 2D). Similarly, CL-316,243-induced browning was also impaired in mice lacking *Blnc1* in adipocytes (Supplementary Fig. 2). Together, these results indicate that *Blnc1* is indispensable for cold-induced thermogenesis and white fat browning.

3.3. Adipocyte-specific inactivation of *Blnc1* exacerbates brown fat whitening and adipose tissue inflammation in obesity

We next examined whether adipocyte-specific inactivation of *Blnc1* accelerates weight gain during HFD feeding. To our surprise, while AKO mice gained slightly more weight than control, we did not observe statistically significant differences in body weight between two groups (Figure 2E). Despite this, AKO mice had elevated blood glucose and plasma insulin concentrations following HFD feeding (Figure 2F).

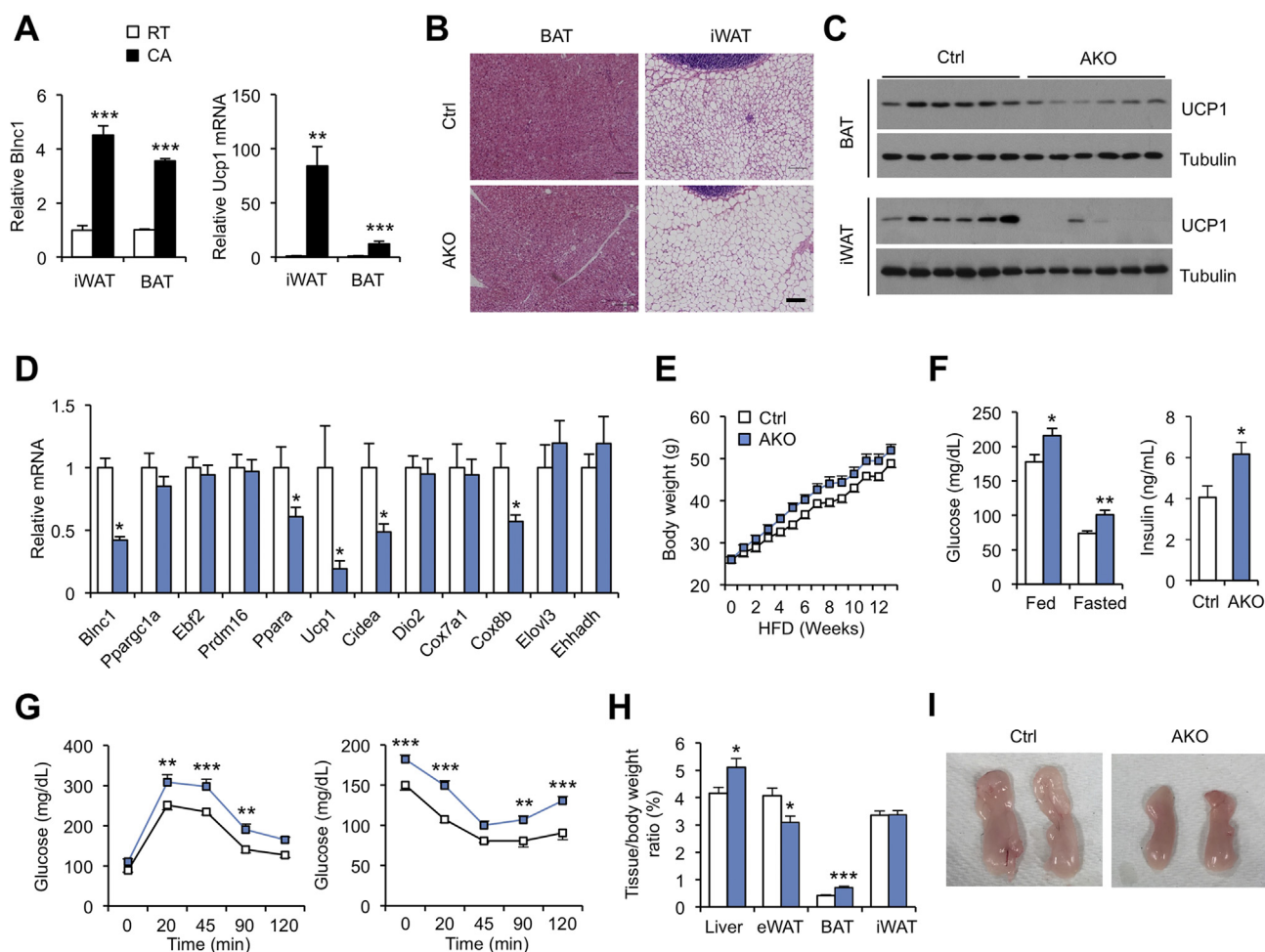


Figure 2: Fat-specific *Blnc1* inactivation impairs thermogenesis and exacerbates diet-induced insulin resistance. (A) qPCR analysis of *Blnc1* expression in iWAT and BAT in mice housed at ambient room temperature (RT) or cold-acclimated (CA). Data represent mean \pm SEM. **p < 0.01, ***p < 0.001, two-tailed unpaired Student's t-test. (B) BAT and iWAT histology in cold-acclimated mice. Scale bar = 100 μ m. (C) Immunoblots of total BAT and iWAT lysates. (D) qPCR analysis of iWAT gene expression. Data represent mean \pm SEM. *p < 0.05, two-tailed unpaired Student's t-test. (E) Body weight of Ctrl (open, n = 8) and AKO (blue, n = 8) mice fed HFD for 13 weeks. Data represent mean \pm SEM. Ctrl vs. AKO, two-way ANOVA with multiple comparisons. (F) Blood glucose and plasma insulin concentrations in HFD-fed mice. Data represent mean \pm SEM. *p < 0.05, **p < 0.01; Ctrl vs. AKO, two-tailed unpaired Student's t-test. (G) GTT (left) and ITT (right) in mice fed HFD for 8 and 9 weeks, respectively. Ctrl (open, n = 8) and AKO (blue, n = 8). Data represent mean \pm SEM. ***p < 0.01, ****p < 0.0001; Ctrl vs. AKO, two-way ANOVA with multiple comparisons. (H) Tissue weight/body weight ratio in mice fed HFD for 13 weeks. Data represent mean \pm SEM. *p < 0.05, ***p < 0.001; Ctrl vs. AKO, two-tailed unpaired Student's t-test. (I) Images of eWAT in the Ctrl or AKO mice fed HFD for 13 weeks.

Glucose tolerance test (GTT) and insulin tolerance test (ITT) indicated that HFD-fed AKO mice developed more severe glucose intolerance and insulin resistance (Figure 2G). *Blnc1*-deficient mice had significantly enlarged liver and BAT, whereas the size of eWAT appeared smaller (Figure 2H–I). Further, eWAT from HFD-fed AKO mice appeared atrophic, a feature commonly associated with adipose tissue inflammation.

H&E staining revealed that AKO brown fat assumed a histological appearance that resembles white fat, containing large unilocular lipid droplets (Figure 3A). White fat from AKO mice contained abundant crown-like structures that are characteristic of obesity-associated adipose tissue inflammation. Sirius red staining and hydroxyproline measurements indicate that, compared to control, AKO mice developed more severe adipose tissue fibrosis upon HFD feeding (Figure 3A–B). Adipose tissue dysfunction impairs its ability to store fat and has been linked to the pathogenesis of hepatic steatosis. Consistent with this, we observed significantly higher liver fat content and more severe hepatic steatosis in HFD-fed AKO mice compared to control (Figure 3C).

Recent studies demonstrate that HFD feeding promotes BAT whitening, which is characterized by a loss of the molecular and morphological features of brown fat [20,21]. We next performed gene expression analysis to assess whether *Blnc1* deficiency accelerates HFD-induced BAT whitening. As shown in Figure 3D, mRNA expression of *Ucp1* and a set of genes involved in mitochondrial fuel oxidation and thermogenesis was significantly decreased by *Blnc1* inactivation. Further, immunoblotting analysis revealed that UCP1 protein levels were greatly diminished in brown fat from AKO mice compared to control (Figure 3E). In eWAT, mRNA expression of genes involved in *de novo* lipogenesis (*Srebp1c*, *Fasn*, *Scd1*), lipid storage (*Dgat2*, *Fabp4*, *Cidec*) and catabolism (*Ehhadh*, *Acaa1b*) was significantly reduced by *Blnc1* inactivation (Figure 3F). In contrast, mRNA levels of several macrophage markers, including *Lgals3*, *Clec4d*, *Slc11a1*, *Cpa3*, and *Tnfaip2*, were elevated in eWAT from HFD-fed AKO mice. Phosphorylation of nuclear factor kappa-light-chain-enhancer of activated B cells (NF- κ B) p65 and p38 mitogen-activated protein kinase (MAPK) was also elevated in *Blnc1*-deficient eWAT (Figure 3E). Together, these results demonstrate that fat-specific *Blnc1* inactivation does not significantly alter whole body energy balance. Instead, *Blnc1* deficiency

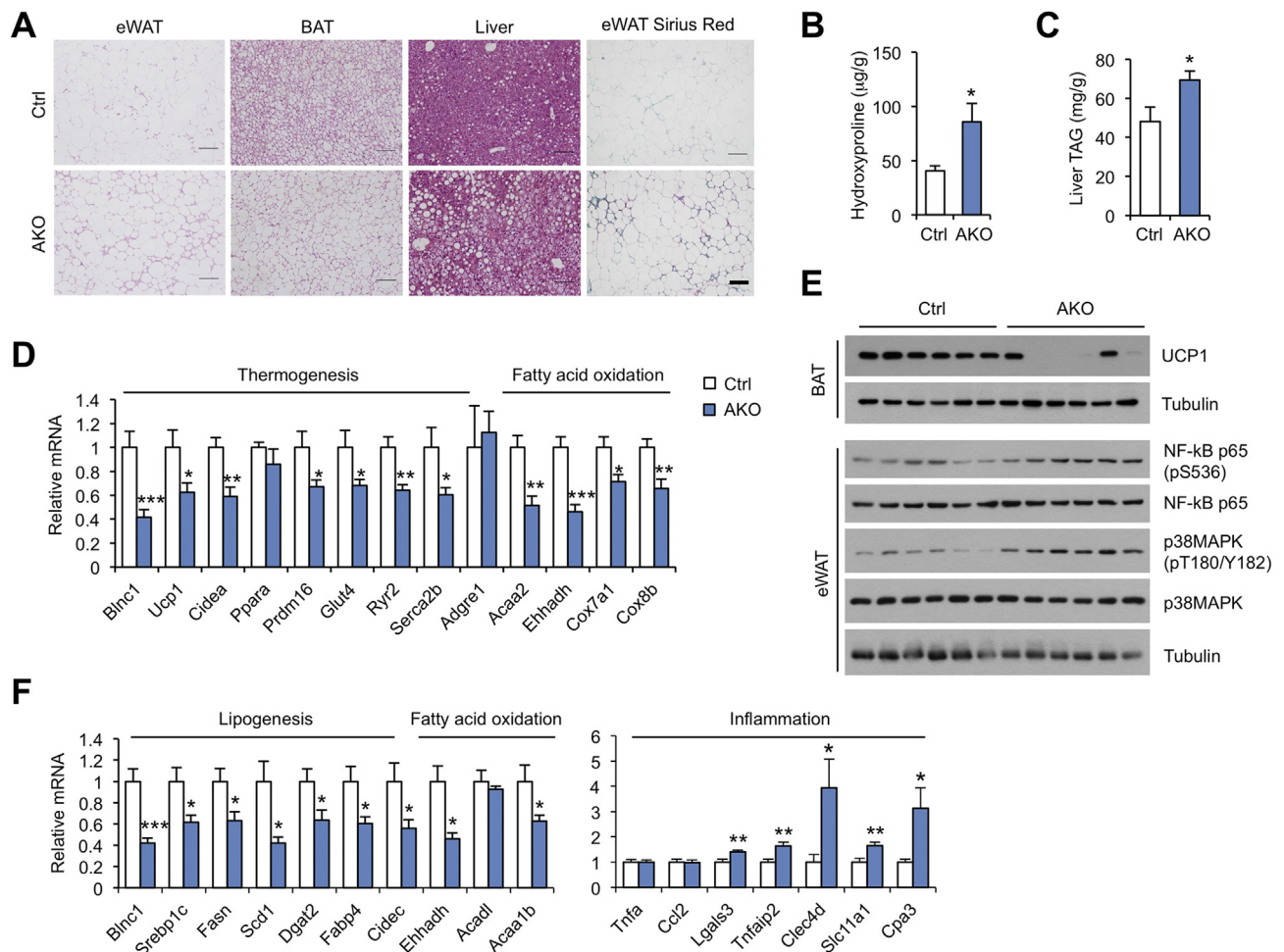


Figure 3: *Blnc1* is required for maintaining adipose tissue homeostasis in obesity. (A) H&E staining of eWAT, BAT and liver sections, and Sirius Red staining of eWAT sections from control (Ctrl) and AKO mice fed HFD for 13 weeks. (B) eWAT hydroxyproline content. (C) Liver triglyceride (TAG) content. Data in B–C represent mean \pm SEM. * $p < 0.05$, Ctrl vs. AKO, two-tailed unpaired Student's *t*-test. (D) qPCR analysis of BAT gene expression. (E) Immunoblots of BAT and eWAT lysates. (F) qPCR analysis of eWAT gene expression. Data in D and F represent mean \pm SEM. * $p < 0.05$, ** $p < 0.01$, *** $p < 0.001$, Ctrl vs. AKO, two-tailed unpaired Student's *t*-test.

exacerbates diet-induced insulin resistance and hepatic steatosis by promoting BAT whitening and eWAT inflammation.

3.4. Fat-specific transgenic expression of *Blnc1* preserves adipose tissue health and systemic metabolic homeostasis

Because *Blnc1* expression in eWAT is significantly elevated in obesity, the metabolic phenotype of *Blnc1* AKO mice strongly suggests that it may coordinate adipose tissue adaptation during obesity. In this regard, *Blnc1* deficiency appears to accelerate whitening of brown fat and worsen obesity-associated inflammation and fibrosis of white fat, leading to systemic metabolic dysregulation. A key prediction of this model is that elevating *Blnc1* levels in adipose tissue will likely protect against adipose tissue dysfunction in obesity and elicit beneficial metabolic effects. To test this, we generated fat-specific *Blnc1* transgenic mice (Tg) with transgenic expression of *Blnc1* restricted to adipose tissue, including BAT, eWAT, and iWAT, but not in tissues containing a large population of resident macrophages, including liver, spleen, and lung (Figure 4A). Unlike some *Fabp4* transgenic strains [41], *Blnc1* Tg mice exhibited undetectable leaky transgenic

expression in adipose tissue macrophages (Figure 4B). *Blnc1* Tg mice exhibited slightly increased UCP1 protein levels in BAT, but not iWAT, when housed at ambient room temperature (Figure 4C). Following cold acclimation, *Blnc1* Tg mice exhibited more pronounced iWAT browning compared to wild type littermates (WT), as revealed by histological staining, UCP1 protein expression, and induction of thermogenic gene markers, including *Ucp1*, *Cidea*, *Cox7a1*, and *Dio2* (Figure 4C–E). We next examined how transgenic expression of *Blnc1* influences adipose tissue adaptation under metabolic stress conditions. We did not observe significant differences in body weight and blood glucose between chow-fed WT and Tg mice. Upon HFD feeding, Tg group exhibited less weight gain for several weeks but this difference disappeared after approximately three months of feeding (Figure 4F). While *ad lib* blood glucose levels were similar, plasma insulin concentrations were significantly lower in Tg mice (Figure 4G). ITT and GTT studies revealed that Tg mice remained more insulin sensitive and glucose tolerant despite continued weight gain that matched WT levels (Figure 4H). While brown fat mass was smaller, eWAT mass was significantly larger in Tg mice and did not exhibit an atrophic

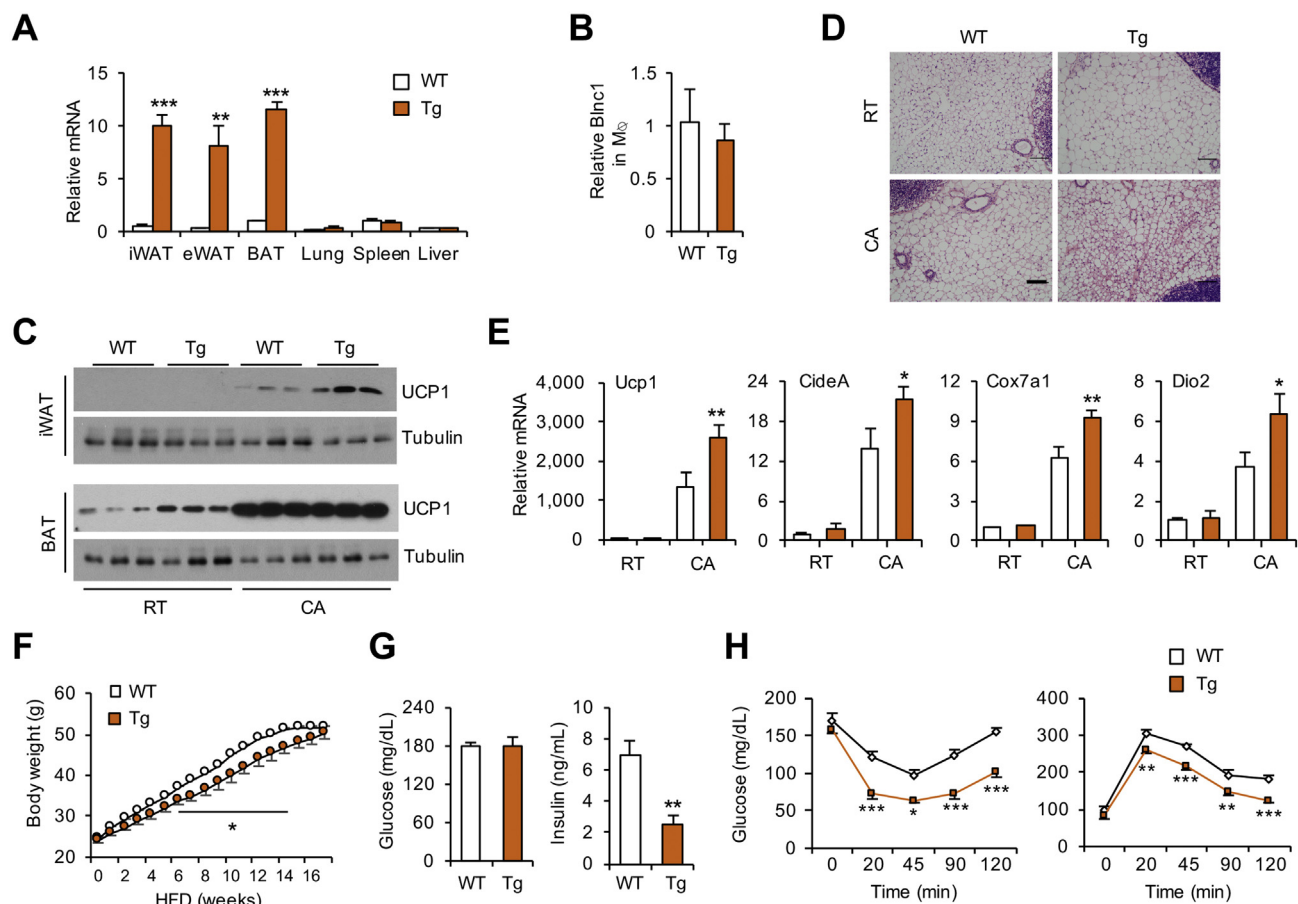


Figure 4: Fat-specific transgenic expression of *Blnc1* preserves metabolic health during HFD feeding. (A) qPCR analysis of *Blnc1* expression in different tissues from WT (open) or *Blnc1* Tg (brown) mice. Data represent mean \pm SD (n = 4). **p < 0.01, ***p < 0.001, WT vs. Tg, two-tailed unpaired Student's t-test. (B) *Blnc1* expression in macrophages from WT and *Blnc1* Tg mouse eWAT. Data represent mean \pm SD (n = 3). WT vs. Tg, two-tailed unpaired Student's t-test. (C) Immunoblots of iWAT or BAT lysates from WT and Tg mice kept at room temperature (RT) or after cold acclimation (CA). (D) H&E staining of iWAT sections. Scale bar = 100 μm. (E) qPCR analysis of iWAT gene expression. WT (open; RT n = 4, CA n = 6) and Tg (brown; RT n = 4, CA n = 8). Data represent mean \pm SEM. *p < 0.05, **p < 0.01 WT vs. Tg, two-way ANOVA. (F) Body weight of WT (open, n = 10) and Tg (brown, n = 7) mice fed HFD for 17 weeks. Data represent mean \pm SEM. *p < 0.05 week 7–14; WT vs. Tg, two-way ANOVA with multiple comparisons. (G) Blood glucose and plasma insulin concentrations. Data represent mean \pm SEM. **p < 0.01; WT vs. Tg, two-tailed unpaired Student's t-test. (H) ITT (left) and GTT (right) in HFD-fed mice. WT (open, n = 6) and Tg (brown, n = 6). Data represent mean \pm SEM. *p < 0.05; **p < 0.01, ***p < 0.001; WT vs. Tg, two-way ANOVA with multiple comparisons.

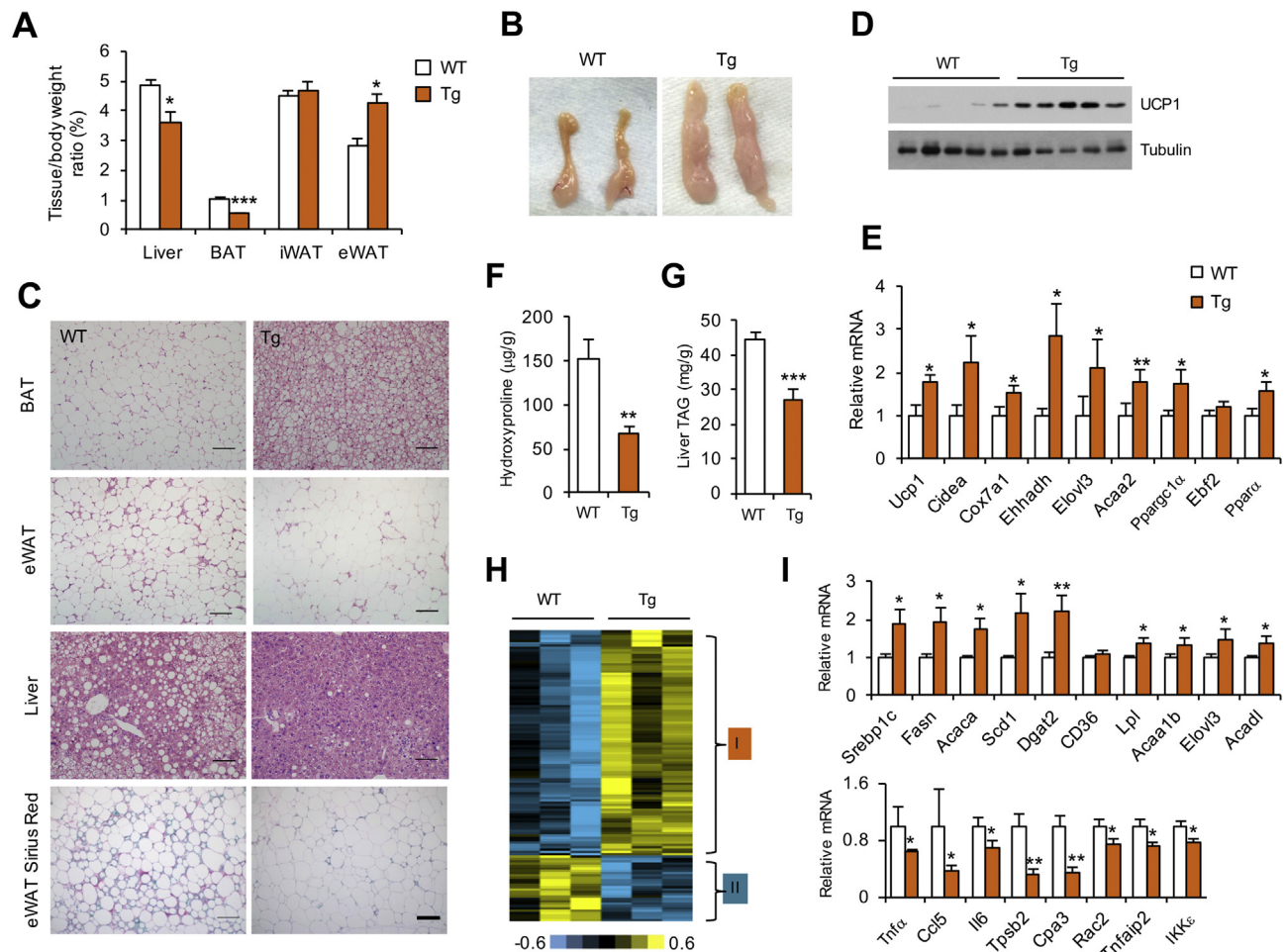


Figure 5: Transgenic expression of *Blnc1* attenuates obesity-associated BAT whitening and eWAT inflammation. (A) Tissue weight/body weight ratio in WT (open, $n = 8$) and Tg (brown, $n = 6$) mice fed HFD for 21 weeks. Data represent mean \pm SEM. * $p < 0.05$, *** $p < 0.001$; WT vs. Tg, two-tailed unpaired Student's *t*-test. (B) Morphology of eWAT from HFD-fed mice. (C) H&E staining of BAT, eWAT and liver sections and Sirius red staining of eWAT sections. Scale bar = 100 μ m. (D) Immunoblots of BAT lysates. (E) qPCR analysis of BAT gene expression. (F) eWAT hydroxyproline content. (G) Liver TAG content. Data in E-G represent mean \pm SEM. * $p < 0.05$, ** $p < 0.01$, *** $p < 0.001$; WT vs. Tg two-tailed unpaired Student's *t*-test. (H) Heat map representation of genes that were upregulated (cluster I) or downregulated (cluster II) in *Blnc1* transgenic eWAT. (I) qPCR analysis of eWAT gene expression. Data represent mean \pm SEM. * $p < 0.05$, ** $p < 0.01$, WT vs. Tg, two-tailed unpaired Student's *t*-test.

appearance, as observed in eWAT WT mice following prolonged HFD feeding (Figure 5A–B). H&E staining revealed that brown fat from transgenic mice had less fat accumulation with lipid droplets assuming multilocular phenotype (Figure 5C). Brown fat UCP1 protein levels and thermogenic gene expression were markedly higher in Tg mice than control (Figure 5D–E), suggesting that transgenic expression of *Blnc1* suppressed whitening of brown fat following diet-induced obesity. Remarkably, eWAT from HFD-fed Tg mice exhibited drastically reduced crown-like structures and less fibrosis (Figure 5C,F). In striking contrast to AKO mice, fat-specific transgenic expression of *Blnc1* decreased liver weight to body weight ratio, reduced hepatic fat content and improved hepatic steatosis (Figure 5G).

We next performed microarray transcriptional profiling to determine the effects of *Blnc1* on global gene expression in eWAT following diet-induced obesity. We identified two clusters of upregulated and downregulated genes in both tissues (Figure 5H). DAVID analysis of gene ontology indicated that genes upregulated by *Blnc1* in eWAT were enriched for lipid metabolism and substrate oxidation, whereas those downregulated were enriched for cytokine production and inflammatory immune response (Supplementary Fig. 3A). qPCR analysis

confirmed that mRNA expression of genes involved in lipogenesis and lipid storage (*Fasn*, *Acaca*, *Scd1* and *Dgat2*) was elevated in transgenic eWAT (Figure 5I), suggesting that *Blnc1* may promote nutrient storage in white fat. In contrast, mRNA levels of a set of genes involved in proinflammatory signaling were significantly downregulated by transgenic *Blnc1*. These results illustrate that transgenic expression of *Blnc1* is sufficient to promote beneficial metabolic adaptation in adipose tissue under chronic nutrient excess conditions.

3.5. *Blnc1* attenuates TNF α signaling and proinflammatory cytokine release in a cell-autonomous manner

We next examined molecular markers of proinflammatory cytokine signaling in WT and Tg eWAT from HFD-fed mice. Compared to WT, the levels of phosphorylated NF- κ B p65 and p38 MAPK were significantly reduced in eWAT from transgenic mice (Supplementary Fig. 3B), whereas total NF- κ B p65 and p38 MAPK protein levels were similar between two groups. Protein levels of IKK ϵ , a noncanonical IKK elevated in white fat during obesity [42], were reduced in transgenic adipose tissue lysates. To further investigate how *Blnc1* transgenic expression modulates cytokine signaling in adipose tissue, we treated

eWAT explant culture isolated from Blnc1 WT and Tg mice with TNF α , a prototypical cytokine associated with adipose tissue inflammation, and examined downstream response. As expected, TNF α treatment potentially stimulated the expression of several known target genes of TNF α , including *Il6*, *Ccl5*, and *Ikk ϵ* and *Tnfaip2* (Supplementary Fig. 3C–3D). In contrast, TNF α response was markedly blunted in eWAT explant from Blnc1 Tg mice.

To determine whether Blnc1 modulates inflammatory signaling in a cell-autonomous manner, we used retroviral vectors to overexpress or knock down Blnc1 expression in C3H10T1/2 adipocytes. Blnc1 overexpression did not affect differentiation of C3H10T1/2 preadipocytes toward white adipocytes. While baseline TANK-binding kinase 1 (TBK1), NF- κ B p65 and p38 MAPK phosphorylation appeared similar, TNF α -induced phosphorylation of these factors was attenuated in adipocytes overexpressing Blnc1 (Figure 6A). Consistently, the induction of *Il6*, *Ccl5*, *Ikk ϵ* , and *Tnfaip2* in response to TNF α was also significantly diminished (Figure 6B). The secretion of CCL5 and IL-6 into adipocyte media was also reduced by retroviral Blnc1 overexpression (Figure 6C). In contrast, RNAi knockdown of Blnc1 rendered C3H10T1/2 adipocytes hyper-responsive to TNF α , leading to increased

phosphorylation of TBK1, NF- κ B p65, and p38 MAPK (Figure 6D), and augmented induction of *Il6*, *Ccl5*, *Ikk ϵ* , and *Tnfaip2* (Figure 6E). ELISA measurements indicated that RNAi knockdown of Blnc1 further enhanced the secretion of CCL5 and IL-6 into culture media following TNF α stimulation (Figure 6F). These gain- and loss-of-function studies illustrate a cell-autonomous mechanism through which Blnc1 attenuates TNF α signaling and cytokine induction in adipocytes.

3.6. Zbtb7b mediates the inhibitory effects of Blnc1 on proinflammatory signaling

We recently identified Zbtb7b, a zinc finger and BTB domain containing transcription factor, as a protein partner for Blnc1 in adipocytes [31]. Zbtb7b stimulates the expression of thermogenic genes and is required for cold-induced thermogenesis and white fat browning. Because Zbtb7b and Blnc1 exhibit strikingly similar effects on adipocyte gene regulation, we postulated that Blnc1 may interact with Zbtb7b to exert its effects on proinflammatory signaling in adipocytes. To test this, we examined proinflammatory cytokine signaling in adipocytes differentiated from C3H10T1/2 fibroblasts transduced with vector or ZBTB7B retrovirus. As shown in Figure 7A, retroviral ZBTB7B overexpression

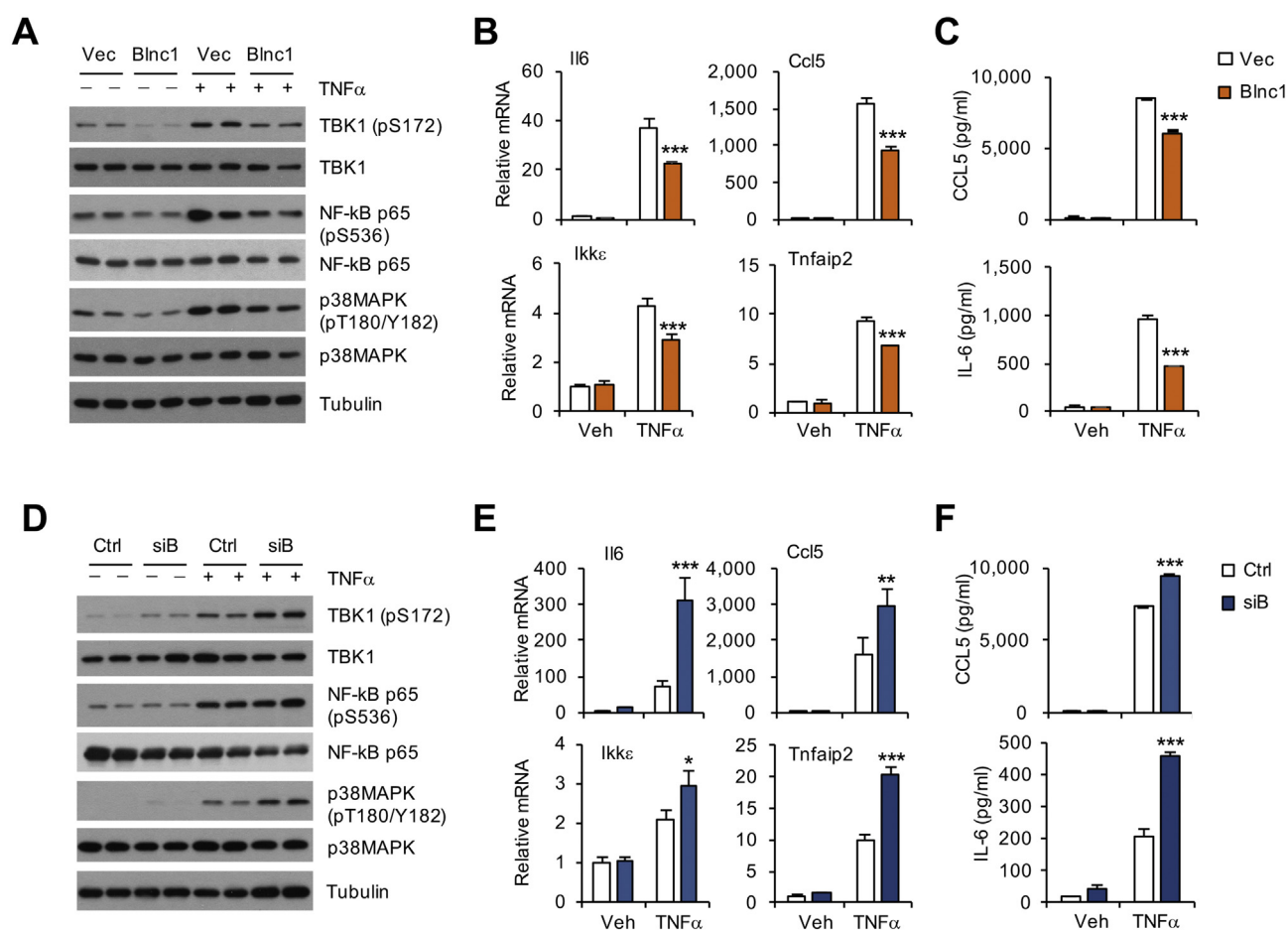


Figure 6: Blnc1 cell-autonomously suppresses TNF α signaling in adipocytes. (A) Immunoblots of total lysates from C3H10T1/2 adipocytes treated with vehicle (–) or 10 ng/ml TNF α for 15 min. (B) qPCR analysis of gene expression in adipocytes treated with vehicle (Veh) or 10 ng/ml TNF α for 24 h. Data represent mean \pm SD (n = 3). ***p < 0.001, Vec vs. Blnc1, two-way ANOVA. (C) Concentrations of cytokines in culture media from treated adipocytes in (B). Data represent mean \pm SD (n = 3). ***p < 0.001, Vec vs. Blnc1, two-way ANOVA. (D) Immunoblots of total lysates from C3H10T1/2 adipocytes expressing control (Ctrl) or shRNA targeting Blnc1 (siB) treated with vehicle (–) or 10 ng/ml TNF α for 15 min. (E) qPCR analysis of gene expression in adipocytes treated with vehicle (Veh) or 10 ng/ml TNF α for 24 hr. Data represent mean \pm SD (n = 3). *p < 0.05, **p < 0.01, ***p < 0.001, Ctrl vs. siB, two-way ANOVA. (F) Concentrations of cytokines in culture media from treated adipocytes in (E). Data represent mean \pm SD (n = 3). ***p < 0.001, Ctrl vs. siB, two-way ANOVA.

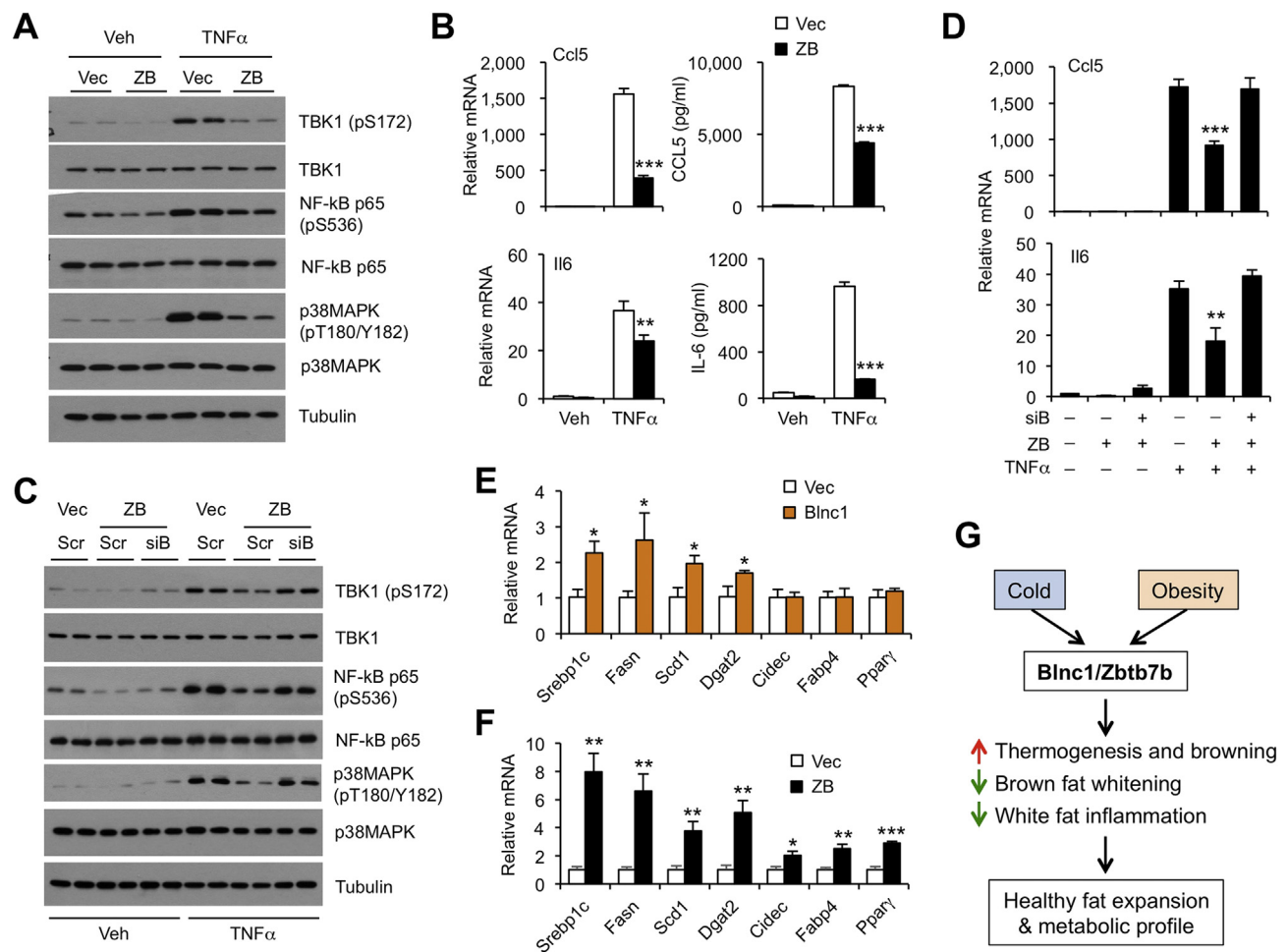


Figure 7: Zbtb7b mediates the inhibitory effects of Blnc1 on proinflammatory signaling. (A) Immunoblots of total lysates from differentiated C3H10T1/2 adipocytes expressing vector (Vec) or Zbtb7b (ZB) treated with vehicle (–) or 10 ng/ml TNF α for 15 min. (B) qPCR of gene expression (left) and cytokines release in culture media (right) in C3H10T1/2 adipocytes treated with vehicle (Veh) or 10 ng/ml TNF α for 24hr. Data represent mean \pm SD (n = 3). **p < 0.01, ***p < 0.001, Vec vs. ZB, two-way ANOVA. (C) Immunoblots of lysates from C3H10T1/2 adipocytes expressing vector (Vec) or Zbtb7b (ZB) in combination with control (Scr) or shRNA targeting Blnc1 (siB) treated with vehicle (–) or 10 ng/ml TNF α for 15 min. (D) qPCR analysis of gene expression in C3H10T1/2 adipocytes expressing vector (Vec) or Zbtb7b (ZB) together with control (Scr) or shRNA targeting Blnc1 (siB) treated with vehicle (–) or 10 ng/ml TNF α for 24hr. Data represent mean \pm SD (n = 3). **p < 0.01, ***p < 0.001, Scr vs. siB, two-way ANOVA. (E–F) qPCR analysis of gene expression in C3H10T1/2 adipocytes transduced with vector, Blnc1 (E) or ZBTB7B (F). Data represent mean \pm SD (n = 3). *p < 0.05, **p < 0.01, ***p < 0.001, two-tailed unpaired Student's t-test. (G) A model depicting the role of the Blnc1/Zbtb7b ribonucleoprotein complex in driving adaptive adipose tissue remodeling and preserving metabolic health.

greatly diminished TNF α -induced phosphorylation of TBK1, NF- κ B p65 and p38 MAPK. Compared to control, mRNA expression and secretion of CCL5 and IL-6 were significantly decreased by ZBTB7B (Figure 7B). To further determine whether Blnc1 is required for the inhibitory effects of ZBTB7B on TNF α signaling, we performed RNA knockdown of Blnc1 in combination with ZBTB7B overexpression. Compared to vector, siRNA knockdown of Blnc1 largely abolished the inhibitory effects of ZBTB7B on inflammatory signaling, cytokine gene expression and secretion (Figure 7C–D).

As shown in Figure 3F, inactivation of Blnc1 in adipocytes significantly decreased the expression of genes involved in lipid synthesis and storage. In contrast, transgenic Blnc1 expression augmented the expression of this cluster of genes (Figure 5I). These findings strongly suggest that Blnc1 facilitates fuel storage and health white fat expansion. In support of this, retroviral overexpression of Blnc1 and ZBTB7B stimulated the expression of genes involved in *de novo* lipogenesis and triglyceride synthesis

(Figure 7E–F). These data illustrate a cell-autonomous role of the ZBTB7B/Blnc1 ribonucleoprotein complex in suppressing proinflammatory signaling and promoting fuel storage in adipocytes.

4. DISCUSSION

The recognition of widespread transcription beyond protein-coding genes in the genome led to the discovery of functional lncRNAs with diverse biological activities. By performing unbiased transcriptomic analyses, several recent studies have cataloged lncRNAs that exhibit differential expression in brown and white fats and inducible expression during adipocyte differentiation [37–39]. To date, functional studies of adipose lncRNAs have been limited to cultured adipocytes and their significance in adipose tissue homeostasis, metabolism and physiology remains uncertain. In this study, we generated fat-specific Blnc1 knockout and transgenic mouse strains and interrogated its role in

adipose adaptation to cold temperature and chronic nutrient excess. Our studies uncovered a surprisingly pleiotropic and dominant role of lncRNA in promoting adaptive adipose tissue remodeling and preserving systemic metabolic health (Figure 7G).

A somewhat unexpected initial finding was that obesity increased Blnc1 expression in brown fat. Recent studies have demonstrated that brown adipocytes acquire white adipocyte-like phenotype upon prolonged HFD feeding, a process termed whitening. Brown fat whitening is characterized by marked fat accumulation and the presence of unilocular lipid droplets in brown adipocytes [19,21]. These morphological changes are associated with suppression of the brown fat gene program and induction of WAT-enriched genes. We previously demonstrated that Blnc1 promotes thermogenic gene expression during brown and beige adipocyte differentiation [39]. As such, increased BAT Blnc1 expression may serve as a checkpoint to maintain the molecular and functional characteristics of brown fat and restrict obesity-associated whitening. Several lines of evidence support this model. First, Blnc1 is required for cold-induced thermogenesis; fat-specific inactivation of Blnc1 rendered AKO mice highly cold-intolerant. Further, AKO mice failed to fully activate the program of iWAT browning following cold acclimation or adrenergic activation. Importantly, adipocyte-specific transgenic expression of Blnc1 was sufficient to augment iWAT browning in cold-acclimated mice. A direct role of Blnc1 in attenuating brown fat whitening is illustrated by the HFD feeding studies. Blnc1 deficiency greatly accelerated the morphological and molecular hallmarks associated with whitening of brown adipocytes, whereas elevating Blnc1 levels elicited an opposite effect in brown fat from Blnc1 transgenic mice in the context of diet-induced obesity. These results illustrate dual role of Blnc1 in driving cold-induced thermogenesis and restricting obesity-associated brown fat whitening.

Expansion of white fat mass is an important aspect of adipose tissue remodeling and organismal adaptation to chronic positive energy balance [1,3]. The marked increase in fat mass during obesity results from a combination of adipocyte hypertrophy and generation of new adipocytes from progenitor cells. While the exact mechanisms remain unknown, it has been recognized that fat expansion can transition into a pathophysiological state that is characterized by local inflammation and fibrosis. The latter is strongly associated with systemic insulin resistance and ectopic fat accumulation in other peripheral tissues, such as the liver. The remarkable induction of Blnc1 expression in eWAT from diet-induced and genetic obese mice raised an intriguing possibility that this lncRNA may regulate adipose biology beyond its effects on thermogenesis. In fact, we did not observe robust effects of Blnc1 inactivation and transgenic expression on HFD-induced weight gain, suggesting that the metabolic phenotype of Blnc1 AKO and Tg mice cannot be fully explained by its effects on thermogenesis and energy expenditure. In support of this, we observed that Blnc1 inactivation impairs white fat expansion during HFD feeding. Despite having similar diet-induced weight gain, AKO mice had smaller eWAT mass compared to control and exhibited decreased expression of genes involved in lipid synthesis and storage. In addition, HFD-fed AKO mice exhibited more severe adipose tissue inflammation and fibrosis, leading to hepatic steatosis and insulin resistance. These loss-of-function studies were further supported by observations obtained from transgenic mice. Fat-specific transgenic expression of Blnc1 promotes healthy fat expansion during HFD feeding that is associated with reduced adipose tissue inflammation and fibrosis, and improved systemic metabolic profile.

Our data are consistent with a cell-autonomous role of Blnc1 in the regulation of inflammatory signaling in white adipocytes. Retroviral Blnc1 overexpression suppressed TNF α signaling and cytokine

production in differentiated C3H10T1/2 adipocytes, whereas Blnc1 shRNA knockdown exaggerated the response to TNF α . At the molecular level, Blnc1 acts cooperatively with its protein partner Zbtb7 to regulate cytokine signaling and lipid storage genes in adipocytes. Together, these observations support a more pervasive role of Blnc1 in the regulation of distinct gene programs in white and brown/beige adipocytes. The increased expression of Blnc1 in adipose tissue serves as an adaptive mechanism to promote healthy adipose tissue remodeling and maintain metabolic homeostasis during obesity. This work provides compelling *in vivo* evidence that lncRNAs are critical and powerful regulators of adipose tissue metabolism and physiology.

ACKNOWLEDGMENTS

This work was supported by NIH (DK102456, J.D.L.), American Diabetes Association (1-15-BS-118, J.D.L.), and a pilot grant from the Michigan Nutrition Obesity Research Center (P30DK089503, S.L.). L.M. was supported by a predoctoral fellowship from the Chinese Scholarship Council (201506300141). X.Y.Z. was supported by NIH Pathway to Independence Award (DK106664). This work used core services supported by the Michigan Diabetes Research Center and the Michigan Nutrition and Obesity Research Center (NIH grants P30-DK020572 and P30-DK089503).

DECLARATION OF INTERESTS

The authors declare no conflict of interest.

AUTHOR CONTRIBUTIONS

X.Y.Z. and J.D.L. conceived the project and designed research. X.Y.Z., J.L.D., T.L., S.L., M.L. and X.P. performed the studies. X.Y.Z. J.D.L. and C.N.L. analyzed the data and wrote the manuscript.

APPENDIX A. SUPPLEMENTARY DATA

Supplementary data related to this article can be found at <https://doi.org/10.1016/j.molmet.2018.06.005>.

REFERENCES

- [1] Crewe, C., An, Y.A., Scherer, P.E., 2017. The ominous triad of adipose tissue dysfunction: inflammation, fibrosis, and impaired angiogenesis. *Journal of Clinical Investigation* 127:74–82.
- [2] Gregor, M.F., Hotamisligil, G.S., 2011. Inflammatory mechanisms in obesity. *Annual Review of Immunology* 29:415–445.
- [3] Martinez-Santibanez, G., Lumeng, C.N., 2014. Macrophages and the regulation of adipose tissue remodeling. *Annual Review of Nutrition* 34:57–76.
- [4] Odegaard, J.I., Chawla, A., 2013. Pleiotropic actions of insulin resistance and inflammation in metabolic homeostasis. *Science* 339:172–177.
- [5] Rosen, E.D., Spiegelman, B.M., 2014. What we talk about when we talk about fat. *Cell* 156:20–44.
- [6] Saltiel, A.R., Olefsky, J.M., 2017. Inflammatory mechanisms linking obesity and metabolic disease. *Journal of Clinical Investigation* 127:1–4.
- [7] Cannon, B., Nedergaard, J., 2004. Brown adipose tissue: function and physiological significance. *Physiological Reviews* 84:277–359.
- [8] Harms, M.J., Ishibashi, J., Wang, W., Lim, H.W., Goyama, S., Sato, T., et al., 2014. Prdm16 is required for the maintenance of brown adipocyte identity and function in adult mice. *Cell Metabolism* 19:593–604.

- [9] Kajimura, S., Spiegelman, B.M., Seale, P., 2015. Brown and beige fat: physiological roles beyond heat generation. *Cell Metabolism* 22:546–559.
- [10] Wang, G.X., Zhao, X.Y., Lin, J.D., 2015. The brown fat secretome: metabolic functions beyond thermogenesis. *Trends in Endocrinology and Metabolism* 26: 231–237.
- [11] Villarroya, F., Cereijo, R., Villarroya, J., Giralt, M., 2017. Brown adipose tissue as a secretory organ. *Nature Reviews Endocrinology* 13:26–35.
- [12] Lee, Y.H., Petkova, A.P., Granneman, J.G., 2013. Identification of an adipogenic niche for adipose tissue remodeling and restoration. *Cell Metabolism* 18: 355–367.
- [13] Cipolletta, D., Feuerer, M., Li, A., Kamei, N., Lee, J., Shoelson, S.E., et al., 2012. PPAR- γ is a major driver of the accumulation and phenotype of adipose tissue Treg cells. *Nature* 486:549–553.
- [14] Sun, K., Tordjman, J., Clement, K., Scherer, P.E., 2013. Fibrosis and adipose tissue dysfunction. *Cell Metabolism* 18:470–477.
- [15] Betz, M.J., Enerback, S., 2018. Targeting thermogenesis in brown fat and muscle to treat obesity and metabolic disease. *Nature Reviews Endocrinology* 14:77–87.
- [16] Bartelt, A., Bruns, O.T., Reimer, R., Hohenberg, H., Itrich, H., Peldschus, K., et al., 2011. Brown adipose tissue activity controls triglyceride clearance. *Nature Medicine* 17:200–205.
- [17] Yoneshiro, T., Aita, S., Matsushita, M., Kayahara, T., Kameya, T., Kawai, Y., et al., 2013. Recruited brown adipose tissue as an antiobesity agent in humans. *The Journal of Clinical Investigation* 123:3404–3408.
- [18] Hanssen, M.J., Hoeks, J., Brans, B., van der Lans, A.A., Schaart, G., van den Driessche, J.J., et al., 2015. Short-term cold acclimation improves insulin sensitivity in patients with type 2 diabetes mellitus. *Nature Medicine* 21: 863–865.
- [19] Duteil, D., Tomic, M., Lausecker, F., Nenseth, H.Z., Muller, J.M., Urban, S., et al., 2016. Lsd1 ablation triggers metabolic reprogramming of Brown adipose tissue. *Cell Reports* 17:1008–1021.
- [20] Mori, M.A., Thomou, T., Boucher, J., Lee, K.Y., Lallukka, S., Kim, J.K., et al., 2014. Altered miRNA processing disrupts brown/white adipocyte determination and associates with lipodystrophy. *Journal of Clinical Investigation* 124: 3339–3351.
- [21] Shimizu, I., Arahamian, T., Kikuchi, R., Shimizu, A., Papanicolaou, K.N., MacLachlan, S., et al., 2014. Vascular rarefaction mediates whitening of brown fat in obesity. *Journal of Clinical Investigation* 124:2099–2112.
- [22] Chen, Z., Wang, G.X., Ma, S.L., Jung, D.Y., Ha, H., Altamimi, T., et al., 2017. Nrg4 promotes fuel oxidation and a healthy adipokine profile to ameliorate diet-induced metabolic disorders. *Molecular Metabolism* 6:863–872.
- [23] Guo, L., Zhang, P., Chen, Z., Xia, H., Li, S., Zhang, Y., et al., 2017. Hepatic neuregulin 4 signaling defines an endocrine checkpoint for steatosis-to-NASH progression. *Journal of Clinical Investigation* 127:4449–4461.
- [24] Wang, G.X., Zhao, X.Y., Meng, Z.X., Kern, M., Dietrich, A., Chen, Z., et al., 2014. The brown fat-enriched secreted factor Nrg4 preserves metabolic homeostasis through attenuation of hepatic lipogenesis. *Nature Medicine* 20:1436–1443.
- [25] Cohen, P., Levy, J.D., Zhang, Y., Frontini, A., Kolodin, D.P., Svensson, K.J., et al., 2014. Ablation of PRDM16 and beige adipose causes metabolic dysfunction and a subcutaneous to visceral fat switch. *Cell* 156:304–316.
- [26] Seale, P., Kajimura, S., Yang, W., Chin, S., Rohas, L.M., Uldry, M., et al., 2007. Transcriptional control of brown fat determination by PRDM16. *Cell Metabolism* 6:38–54.
- [27] Rajakumari, S., Wu, J., Ishibashi, J., Lim, H.W., Giang, A.H., Won, K.J., et al., 2013. EBF2 determines and maintains brown adipocyte identity. *Cell Metabolism* 17:562–574.
- [28] Kong, X., Banks, A., Liu, T., Kazak, L., Rao, R.R., Cohen, P., et al., 2014. IRF4 is a key thermogenic transcriptional partner of PGC-1 α . *Cell* 158:69–83.
- [29] Dempersmier, J., Sambeat, A., Gulyaeva, O., Paul, S.M., Hudak, C.S., Raposo, H.F., et al., 2015. Cold-inducible Zfp516 activates UCP1 transcription to promote browning of white fat and development of brown fat. *Molecular Cell* 57:235–246.
- [30] Ohno, H., Shinoda, K., Ohyama, K., Sharp, L.Z., Kajimura, S., 2013. EHMT1 controls brown adipose cell fate and thermogenesis through the PRDM16 complex. *Nature* 504:163–167.
- [31] Li, S., Mi, L., Yu, L., Yu, Q., Liu, T., Wang, G.X., et al., 2017. Zbtb7b engages the long noncoding RNA Blnc1 to drive brown and beige fat development and thermogenesis. *Proceedings of the National Academy of Sciences of the U S A* 114:E7111–E7120.
- [32] Zhao, X.Y., Lin, J.D., 2015. Long noncoding RNAs: a new regulatory code in metabolic control. *Trends in Biochemical Sciences* 40:586–596.
- [33] Gupta, R.A., Shah, N., Wang, K.C., Kim, J., Horlings, H.M., Wong, D.J., et al., 2010. Long non-coding RNA HOTAIR reprograms chromatin state to promote cancer metastasis. *Nature* 464:1071–1076.
- [34] Huarte, M., Guttman, M., Feldser, D., Garber, M., Koziol, M.J., Kenzelmann-Broz, D., et al., 2010. A large intergenic noncoding RNA induced by p53 mediates global gene repression in the p53 response. *Cell* 142:409–419.
- [35] Pauli, A., Valen, E., Lin, M.F., Garber, M., Vastenhouw, N.L., Levin, J.Z., et al., 2012. Systematic identification of long noncoding RNAs expressed during zebrafish embryogenesis. *Genome Research* 22:577–591.
- [36] Vollmers, C., Schmitz, R.J., Nathanson, J., Yeo, G., Ecker, J.R., Panda, S., 2012. Circadian oscillations of protein-coding and regulatory RNAs in a highly dynamic mammalian liver epigenome. *Cell Metabolism* 16:833–845.
- [37] Alvarez-Dominguez, J.R., Bai, Z., Xu, D., Yuan, B., Lo, K.A., Yoon, M.J., et al., 2015. De novo reconstruction of adipose tissue transcriptomes reveals long non-coding RNA regulators of Brown adipocyte development. *Cell Metabolism* 21:764–776.
- [38] Sun, L., Goff, L.A., Trapnell, C., Alexander, R., Lo, K.A., Hacisuleyman, E., et al., 2013. Long noncoding RNAs regulate adipogenesis. *Proceedings of the National Academy of Sciences of the U S A* 110:3387–3392.
- [39] Zhao, X.Y., Li, S., Wang, G.X., Yu, Q., Lin, J.D., 2014. A long noncoding RNA transcriptional regulatory circuit drives thermogenic adipocyte differentiation. *Molecular Cell* 55:372–382.
- [40] Mi, L., Zhao, X.Y., Li, S., Yang, G., Lin, J.D., 2017. Conserved function of the long noncoding RNA Blnc1 in brown adipocyte differentiation. *Molecular Metabolism* 6:101–110.
- [41] Lee, K.Y., Russell, S.J., Ussar, S., Boucher, J., Vernochet, C., Mori, M.A., et al., 2013. Lessons on conditional gene targeting in mouse adipose tissue. *Diabetes* 62:864–874.
- [42] Chiang, S.H., Bazuine, M., Lumeng, C.N., Geletka, L.M., Mowers, J., White, N.M., et al., 2009. The protein kinase IKK ϵ regulates energy balance in obese mice. *Cell* 138:961–975.
- [43] Ran, F.A., Hsu, P.D., Wright, J., Agarwala, V., Scott, D.A., Zhang, F., 2013. Genome engineering using the CRISPR-Cas9 system. *Nature Protocols* 8: 2281–2308.
- [44] Graves, R.A., Tontonoz, P., Platt, K.A., Ross, S.R., Spiegelman, B.M., 1992. Identification of a fat cell enhancer: analysis of requirements for adipose tissue-specific gene expression. *Journal of Cellular Biochemistry* 49: 219–224.
- [45] Ma, D., Molusky, M.M., Song, J., Hu, C.R., Fang, F., Rui, C., et al., 2013. Autophagy deficiency by hepatic FIP200 deletion uncouples steatosis from liver injury in NAFLD. *Molecular Endocrinology* 27:1643–1654.
- [46] Li, S., Liu, C., Li, N., Hao, T., Han, T., Hill, D.E., et al., 2008. Genome-wide coactivation analysis of PGC-1 α identifies BAF60a as a regulator of hepatic lipid metabolism. *Cell Metabolism* 8:105–117.